한국수소 및 신에너지 학회 논문집(2003.3), 제14권 제1호
Trans. of the Korean Hydrogen Energy Society (2003.3), Vol. 14, No. 1, pp. 81~95

PSA를 이용한 수소분리 실험과 이론에 관한 연구

최병욱*, 홍성철*, 최대기*, 이병권*, 백영순**, 이창하***
*한국과학기술연구원 환경공정연구부
**한국가스공사 LNG 기술연구센타, ***연세대학교 화학공학과

Experimental and Theoretical study of H_2 Separation Using PSA Process

Byoung-Uk Choi*, Sung-Chul Hong*, Dae-Ki Choi*, Byung-Gwon Lee*,
Young-Soon Baek**, Chang-Ha Lee***
**Environment & Process Technology Division, Korea Institute of Science & Technology*
P.O.Box 131, Cheongryang, Seoul 130-650, Korea
***LNG Technology Research Center, Korea Gas Corporation*
****Department of Chemical Engineering, Yonsei University*

ABSTRACT

본 연구는 압력균등화 공정이 추가된 2 컬럼 6 스텝의 활성탄 PSA공정을 이용하여 비단열, 비등온 조건에서 메탄(80 %)과 수소(20 %)의 2성분계로부터 수소분리에 관한 연구이다. 공급가스의 압력, 흡착시간, 공급속도와 P/F 비율이 PSA공정에 미치는 영향에 대하여 평가했고 전산모사를 통해 최적조건을 구했다. 전산모사에 의한 최적 조건은 공급속도 17 LPM, 흡착압력 11 atm, P/F 비율이 0.07~0.1로 나타났으며, 이 조건으로부터 순도 99 %, 회수율 85 % 이상의 수소가스를 얻을 수 있었다.

주요기술용어 : PSA(PSA), Hydrogen(수소), Adsorption(흡착), Recovery(회수율), Purification (순도)

Nomenclature

A_W : cross sectional area, cm^2
C : concentration of adsorbate, *mol/g*
C_0 : initial concentration of adsorbate, *mol/g*
C_{pg} : gas heat capacity, *Cal/gK*
C_{ps} : particle heat capacity, *Cal/gK*
C_{pw} : bed wall heat capacity, *Cal/gK*
D_k : knudsen diffusivity, cm^2/s
D_L : mass axial dispersion coefficient, cm^2/s
D_m : molecular diffusivity, cm^2/s
D_p : intraparticle diffusivity, cm^2/s
h : heat transfer coefficient, $Cal/cm^2 \cdot s \cdot K$
k : linear driving force mass transfer coefficient, s^{-1}
$k_{1\text{-}6}$: loading ratio correlation isotherm

model parameter
k_f : external film mass transfer coefficient, cm^2/s
k_g : thermal conductivity of fluid, $cal/cm^2 \cdot s \cdot K$
k_s : thermal conductivity of particle, $cal/cm^2 \cdot s \cdot K$
K : equilibrium constant, q^*/C_0, Henry's law adsorption equilibrium constant
K_L : effective axial thermal conductivity, $cal/cm^2 \cdot s \cdot K$
K_{L0} : initial effective axial thermal conductivity, $cal/cm^2 \cdot s \cdot K$
P : pressure, atm
Pr : Pramdtl number, $C_{pg}\mu/k_g$
P_r : reduced pressure
q : equilibrium moles adsorbed, mol/g
q_m : maximum equilibrium moles adsorbed, mol/g
$\bar{q}$: volume-averaged adsorbed phase concentration, mol/g
q^* : equilibrium adsorbed phase concentration, mol/g
Q : average isosteric heat of adsorption, cal/g or volumetric flow rate, cm^3/s
r_p : single particle radius, cm
R : gas constant, $cal/molK$
R_B : bed radius, cm
R_P : particle radius, cm
Re : Reynolds number, $\rho_g v(2R_P)/\mu$
S_C : Schmidt number, $\mu/\rho_g D_m$
t : time, s
T : temperature, K
T_{atm} : ambient temperature, K
T_w : wall temperature, K
u : interstitial velocity, cm/s
u_0 : initial interstitial velocity, cm/s
y : mole fraction in gas phase
Z : axial position in a adsorption bed, cm

Greek letters

ε : interparticle void fraction
ε_t : total void fraction
ρ_B : bulk density, cm^3/g
ρ_g : gas density, cm^3/g
ρ_p : particle density, cm^3/g
ρ_w : bed density, cm^3/g
δ : parameters used in Eq.(7)
φ : parameters used in Eq.(8)
τ : tortuosity factor

1. Introduction

Environmental regulations have been restricted and crude oil will be run dry in the future. Therefore, many researchers have been interested in hydrogen since hydrogen is regarded as an ecologically clean and renewable energy source, and recent demands for high purity hydrogen are on the rise from utilization in such fields as fuel cell, semiconductor processing and the petrochemical industry. Recently, natural gas pyrolysis and plasma reaction processes, CO_2-free processes, in anoxic environment have studied to produce hydrogen. Although they do not emit carbon dioxide, it is still required separation process to separate high purity hydrogen since their product includes impurities. To separate high purity hydrogen from these products, the pressure swing adsorption(PSA) technology is attractive for its low energy requirements and low capital investment costs. It is based on the physical phenomenon that the amount of a species adsorbed by an adsorbent increases as its partial pressure is raised. Regeneration of the adsorbent during desorption cycle is also achieved simply by reducing the total pressure and purging the bed at low pressure with a small fraction of the product stream[1,2].

Since the introduction of the Skarstrom

cycle[3], the first major improvement to the PSA process was the introduction of the pressure equalization step[4,5]. Pressure equalization allows a significant saving in overall process energy consumption since less mechanical energy is required to repressurize the purged, low-pressure bed. The other major improvement to the PSA process was the introduction of multiple beds[6~8]. The increases number of beds allows a greater number of pressure equalization steps, thereby reducing the amount of feed or product gas required for bed repressurization. This results in a tremendous increase in the product recovery, and a further reduction in mechanical energy consumption at the expense of somewhat higher capital cost. Other modifications to the PSA are the set of multiple adsorbents[6,9,10,11], and the use of the backfill step in a two-bed process that allowed product to be obtained while the other bed was being partially repressurized[12~13]. In this study, two-bed six-step PSA process including pressure equalization step was considered.

Adsorption modeling for a fixed bed system has been extensively studied for both isothermal[14~16] and nonisothermal systems [17,18,19]. Most of the models presented assume that the gas, regarded as ideal, is in the plug flow or plug flow with axial dispersion. The radial concentration and temperature gradients are neglected. The adsorption equilibrium is described using multicomponent isotherms, only rarely have the linear isotherms been used. The gas-solid mass transport is usually modeledby the linear driving force(LDF) approximation[7]. Especially, Malek and Farooq[8,9,20], Harwell et al[21] and Wong et al[22] used a constant LDF mass-transfer coefficient. They stated that it was particularly beneficial to model a multibed, multicomponent pressure swing adsorption process for hydrogen purification. In this study, axially dispersed plug flow model was adopted and the linear driving force(LDF) approximation was used. Also, a complete nonisothermal and nonadiabatic dynamic model is adopted considering energy balance because heat of adsorption and desorption cause temperature variation, 20-40K. Generally, the influence of nonisothermal behavior in PSA process is to reduce the separation performance versus that obtainable from isothermal conditions because the nonisothermal case leads to adsorption at higher temperature and desorption at lower temperature, both of which reduce efficiency. Reliable adsorption equilibrium data is crucial since the isotherms so derived generally form the basis for further adsorption process design and engineering. Especially, high pressure range single and multicomponent adsorption equilibrium data is needed to separate some component using the pressure swing adsorption process. However, due to the substantial amount of time involved in conducting related experiments, there is scant published data on the mixtures. The mixture isotherm data thus are not usually obtained directly, but through correlated single component isotherms[23~25]. Therefore the Langmuir-Fruendlich(L-F) isotherm was adopted for single component adsorption equilibrium and then it extended to loading ratio correlation(LRC) model for multicomponent. Efficient performance of a pressure swing adsorption unit depends on achieving the correct combination of process variables such as bed length, flow rate, cycle

time, pressure ratio and purge-to-feed(P/F) ratio. The effects of these variables are coupled so that it is difficult to arrive at an optimal designing simply by intuition and empiricism. Only P/F raio, adsorption pressure and feed rate effects were considered in this study.

2. Mathematical model for non-isothermal and nonadiabatic bed

The following assumptions were considered in this study.

1) The ideal gas law applies.
2) The flow pattern in the bed can be described by the axial dispersion plug flow model.
3) The solid and gas phase reach thermal equilibrium instantaneously.
4) Radial concentration and temperature gradients on the adsorption bed are negligible.
5) Axial conduction in the wall can be neglected.
6) The mass transfer rate is represented by a linear driving force expression.
7) The multicomponent adsorption equilibrium is represented by the loading ratio correlation.

2.1 Material balance

Using the flow pattern described by axial dispersion plug flow, the material balance for the bulk phase in the adsorption column is given by

$$-D_L\frac{\partial^2 C_i}{\partial z^2}+\frac{\partial uC_i}{\partial z}+\frac{\partial C_i}{\partial t}+\frac{1-\varepsilon}{\varepsilon}\rho_p\frac{\partial q}{\partial t}=0 \quad (1)$$

and overall mass balance can be written as:

$$-D_L\frac{\partial^2 C}{\partial z^2}+\frac{\partial uC}{\partial z}+\frac{\partial C}{\partial t}+\frac{1-\varepsilon}{\varepsilon}\rho_p\sum_{i=0}^{n}\frac{\partial \overline{q_i}}{\partial t}=0 \quad (2)$$

where D_L is axial dispersion coefficient. It can be calculated by Wakao Eq.30 and followed:

$$\frac{D_L}{2uR_P}=\frac{20}{ReSc}+0.5 \quad (3)$$

In this model, the effects of all mechanisms which contribute to axial mixing are lumped together into a single effective axial dispersion coefficient, and it is possible to neglect axial dispersion and assume ideal plug model. If ideal gas law applies to these equations, these equations, Eq.(1) and Eq.(2), can be transformed into:

$$-D_L\frac{\partial^2 y}{\partial z^2}+\frac{\partial y_i}{\partial t}+u\frac{\partial y}{\partial z}+\frac{RT}{P}\frac{1-\varepsilon}{\varepsilon}\rho_p \times\left(\frac{\partial \overline{q_i}}{\partial t}-y_i\sum_{i=0}^{n}\frac{\partial \overline{q_i}}{\partial t}\right)=0 \quad (4)$$

$$-D_L\frac{\partial^2 P}{\partial z^2}+\frac{\partial P}{\partial t}+P\frac{\partial u}{\partial z}-PT\left(-D_L\frac{\partial^2(1/T)}{\partial z^2}+\frac{\partial(1/T)}{\partial t}+u\frac{\partial(1/T)}{\partial z}\right)+\frac{1-\varepsilon}{\varepsilon}RT\sum_{i=0}^{n}\frac{\partial \overline{q_i}}{\partial t}=0 \quad (5)$$

2.2 Energy balance

Assuming thermal equilibrium between fluid and particles, the energy balance for the gas and solid phase is given by:

$$-K_L\frac{\partial^2 T}{\partial z^2}+(\varepsilon_t\rho_g C_{pg}\frac{\partial T}{\partial t}+\rho_g C_{pg}\varepsilon u\frac{\partial T}{\partial z} -\rho_B\sum_{i=0}^{n}Q_i\frac{\partial \overline{q_i}}{\partial t}+\frac{2h_i}{R_{B_i}}(T-T_W)=0 \quad (6)$$

where, K_L is the effective axial thermal conductivity used for taking into account effective conduction in the axial direction. It can be estimated using the empirical correlation given by Kunii and Smith[36] and Yagi et al[26] as follows:

$$\frac{K_L}{k_g} = \frac{K_{L_0}}{k_g} + \delta \, \mathrm{Pr} \, \mathrm{Re} \tag{7}$$

$$\frac{K_{L_0}}{k_g} = \varepsilon + \frac{1-\varepsilon}{\varphi + \frac{2}{3}\frac{k_g}{k_s}} \tag{8}$$

$$\varphi = \varphi_2 + (\varphi_1 - \varphi_2)\left(\frac{\varepsilon - 0.216}{0.216}\right) \quad \text{for } 0.260 \leq \varepsilon \geq 0.476 \tag{9}$$

For all the simulations conducted in this study, the following parameter values were adopted[29]:

$$(\delta, \ \varphi_1, \ \varphi_2) = (0.75, \ 0.2, \ 0.1) \tag{10}$$

In Eq.(6), the last term could be neglected causing heat transfer to wall is not significant in comparison with the amount of heat from adsorption, if length-to-diameter is not large. However, since the diameter of the adsorption bed in the present study was rather small, heat loss through wall and heat accumulation in the wall could not be neglected. Therefore, energy balance for the wall of the adsorption bed was constructed with assumption of neglecting axial conduction in the wall:

$$\rho_w C_{Pw} A_w \frac{\partial T_w}{\partial t} = 2\pi R_{B_i} h_i (T - T_w) - 2\pi R_{B_0} h_0 (T - T_{atm}) \tag{11}$$

$$A_w = \pi \left(R_{B_0}^2 - R_{B_0}^2 \right) \tag{12}$$

2.3 Adsorption rate

The sorption rate into an adsorbent pellet is described by the following LDF model, which involves many possible mass transfer phenomena within a porous medium and external mass transfer into a single lumped mass transfer parameter, k [2]

$$\frac{\partial \overline{q_i}}{\partial t} = k_i \left(q_i^* - \overline{q_i} \right) \tag{13}$$

where, q^* is the adsorbed-phase concentration in equilibrium with the local bulk phase concentration, and k is a LDF mass transfer coefficient, which can be estimated by following equation:

$$\frac{1}{Kk} = \frac{R_p}{3k_f} + \frac{R_p^2}{15\,\varepsilon_p\,D_P} + \frac{r_c^2}{15\,K\,D_P} \tag{14}$$

where, Eq.(14) is only applicable when the equilibrium is linear or at least not severely nonlinear and justified by an analysis of the moments of the dynamic response. The external film mass transfer coefficient, k_f, used to calculate film resistance, first term in Eq.(14), was determined using the Wakao and Funazkri relation[28]:

$$Sh = \frac{2R_p K_f}{D_m} = 2.0 + 1.1\,Sc^{1/3}\,\mathrm{Re}^{0.6} \quad \text{for } 0 < \mathrm{Re} < 1000 \tag{15}$$

Second term in Eq.(14), was calculated using the reciprocal addition law expression for molecular and Knudsen diffusion[1]:

$$\frac{1}{D_P} = \tau\left(\frac{1}{D_m} + \frac{1}{D_k}\right) \tag{16}$$

where, τ is the tortuosity factor, which corresponds to straight, randomly oriented, cylindrical pores with equal probability of all possible orientations. The Knudsen and molecular diffusivities were calculated using familiar expressions derived from the kinetic theory of gases [1].

2.4 Adsorption Isotherm

The Langmuir-Fruendlich(L-F) isotherm was adopted for single component adsorption equilibrium and the loading ratio correlation is considered to find proper multicomponent adsorption equilibrium parameters since the only noniterative method is the loading ratio correlation(LRC)[29]:

L-F model: (17)

$$q = \frac{q_m B P^{1/t}}{1 + BP^{1/t}} \tag{17}$$

LRC model :

$$q = \frac{q_m B P^{1/n_i}}{1 + \sum_{j=1}^{n} B_j P_j^{1/n_i}} \tag{18}$$

$$q_{mi} = k1 + k_2 T$$

$$B = k_3 \exp(k_4 / T)$$

$$1/n = k_5 + k_6 / T \tag{19}$$

2.5 Boundary conditions

For a closed-closed system, the Dankwerts boundary conditions are applicable for the component balance. The boundary conditions and the initial conditions used in the PSA simulation are in the following forms.

Boundary conditions at z=0 and z=L for feed pressurization and adsorption steps:

$$-D_L\left(\frac{\partial y_i}{\partial z}\right)\Big|_{z=0} = u(y_i|_{z=0^-} - y_i|_{z=0^+})$$

$$\left(\frac{\partial y_i}{\partial z}\right)\Big|_{z=L} = 0 \tag{20}$$

$$-K_L\left(\frac{\partial T}{\partial z}\right)\Big|_{z=0} = \rho_g C_{pg} u (T|_{z=0^-} - T|_{z=0^+})$$

$$\left(\frac{\partial T}{\partial z}\right)\Big|_{z=L} = 0 \tag{21}$$

Boundary conditions at z=0 and z=L for purge, pressurizing pressure equalization steps:

$$-D_L\left(\frac{\partial y_i}{\partial z}\right)\Big|_{z=L} = u(y_i|_{z=L^+} - y_i|_{z=L^-})$$

$$\left(\frac{\partial y_i}{\partial z}\right)\Big|_{z=0} = 0 \tag{22}$$

$$-K_L\left(\frac{\partial T}{\partial z}\right)\Big|_{z=L} = \rho_g C_{pg} u (T|_{z=L^+} - T|_{z=L^-})$$

$$\left(\frac{\partial T}{\partial z}\right)\Big|_{z=0} = 0 \tag{23}$$

Boundary conditions at z=0 and z=L for depressurizing pressure equalization and countercurrent depressurization steps:

$$\left(\frac{\partial y_i}{\partial z}\right)\Big|_{z=0}=0 \qquad \left(\frac{\partial y_i}{\partial z}\right)\Big|_{z=L}=0 \qquad (24)$$

$$\left(\frac{\partial T}{\partial z}\right)\Big|_{z=0}=0 \qquad \left(\frac{\partial T}{\partial z}\right)\Big|_{z=L}=0 \qquad (25)$$

Velocity boundary condition at z=0 and z=L:

$$u\,|_{z=0}=u_0 \qquad \left(\frac{\partial u}{\partial z}\right)\Big|_{z=L}=0 \qquad (26)$$

Initial condition for saturated bed:

$$C_i(z,\ 0)=C_0 \qquad \overline{q_i}(z,\ 0)=q_i^* \qquad (27)$$

$$T(z,\ 0)=T_{atm} \qquad (28)$$

2.6 Numerical method

A finite difference method(FDM) was used to solve a mathematical model which consisted of coupled partial differential equations. A three-point backward finite difference approximation was used for temporal differential terms in order to improve temporal accuracy. The spatial dimension was discretized by using a second-order central difference and a second-order backward difference for the second-order and the first-order space derivatives, respectively[9,33]. The spatial grid spacing was 1cm, where the time step was 0.02sec. The conversion of model equations into algebraic equations using FDM leads to huge sparse matrix because dependent variables are coupled with each other. As a result, a great deal of computation time is required to solve the problem. In this study, all the partial differential equations were converted into algebraic equations assuming the form of a trigonal matrix and the solutions were obtained by using the method of Doong and Yang[30,31]. Then,

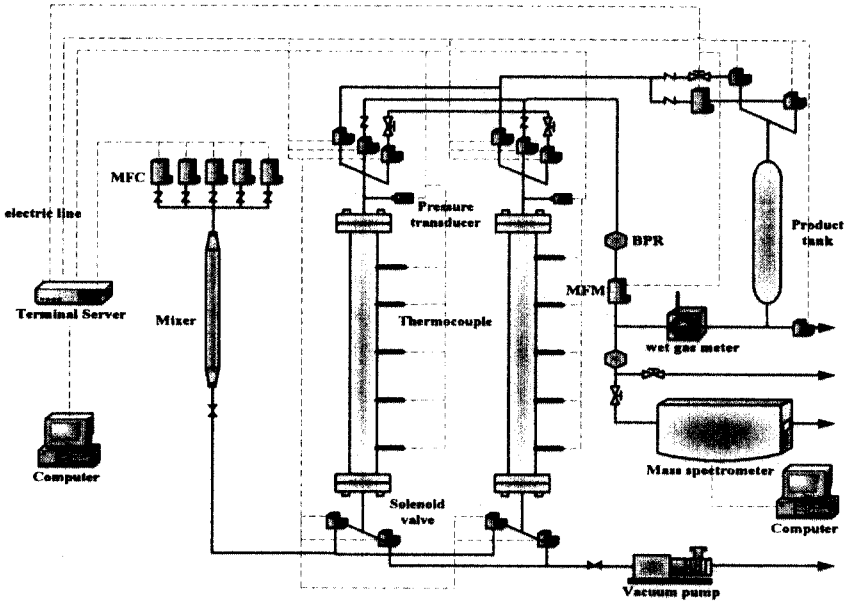

Fig. 1. Schematic diagram of 2-column PSA process apparatus.

Table 1. Characteristics of activated carbon adsorbent.

Length, L[cm]	120
Inside diameter, R_{Bi}[cm]	2.0447
Outside diameter R_{Bo}[cm]	2.2073
Heat capacity of column, C_{pw}[cal/gK]	0.12
Density of column, ρ_w[g/cm^3]	7.83
Internal heat transfer coefficient, h_i[$cal/cm^2 \cdot K \cdot s$]	0.00092
External heat transfer coefficient, h_o[$cal/cm^2 \cdot K \cdot s$]	0.00034

Table 2. Characteristics of adsorption bed

Type	Granular
Nominal pellet size	6-16 mesh
Average pellet size	0.155 mm
Pellet density	0.85 g/cm^3
Heat capacity	0.25 cal/gK
Particle porosity	0.61
Bulk density	0.532 g/cm^3
Bed porosity	0.433
Total void fraction	0.758

computation results were used again through successive substitution until convergence was completed for a given time step. Accordingly, the coupled model equations could be solved in short computation time. The process simulator uses only one bed to simulate two-bed PSA process. To imitate bed connectivities during a pressure equalization step, temporal data of an effluent stream from the adsorption bed undergoing a depressurizing pressure equalization step were retained and used later for the pressurizing pressure equalization step[29].

3. Experimental

3.1 Material

Activated carbon (Calgon Co.) was chosen as an adsorbent. The physical properties tabulated in Table 1 are manufacturer report values. Prior to measurement, the adsorbent was maintained at 423.15K in a drying vacuum oven more than 12h to remove impurities. The adsorbates, and their purity, were methane 99.9% and hydrogen 99.9%.

3.2 Experiment apparatus

A schematic diagram of the 2-column PSA process experimental setup is shown in Fig. 1 and the characteristics of the adsorption column were represented in Table 2. The column was fabricated from stainless steel and was 120cm long with 4.1cm inside diameter. Manual operation might be impossible because PSA process had rapid cycle, and many valves had to be operated simultaneously. So, solenoid valves that could be operated by computer were installed with actuator valve considering high pressure. To control the product flow rate and pressure equalization time, metering valves were installed. The section in both ends of the column was filled with glass wool and metal screen to ensure the uniform gas distribution and prevent the carryover of adsorbent particles. Five K-type thermocouples were installed at 20, 40, 60, 80, and 100cm from end of the column, and the temperature of the system was monitored and saved in DAS(data acquisition system). The gas flow to the column was controlled by a

Table 3. Experiment conditions of 2-column PSA process

Run#	Feed rate [LPM]	Adsorption presuure [atm]	P/F ratio
01	17	11	0.4375
02	17	11	0.0625
03	17	11	0.09375
04	17	11	0.125
05	17	8	0.0625
06	17	9	0.0625
07	17	11	0.0625
08	17	13	0.0625
09	8	11	0.0625
10	11.8	11	0.0625
11	17	11	0.0625
12	21	11	0.0625

mass flow controller(Bronkhorst, Co.) which was precalibrated against a soap bubble flow meter and checked by a wet gas meter. Also, the product flow rate was monitored by mass flow meter (Bronkhorst, Co.) and checked by a wet gas meter. The system total pressure was controlled and maintained at a constant pressure with a electrical back-pressure regulator(Bronkhorst Co.), and was monitored with two pressure-transducers that were installed at each column. The product concentration in the exit stream was detected continuously by mass spectrometer(Balzers, Co.). Also, the feed which was hydrogenand methane(80/20) was premixed by mixer before the feed flow entered into the PSA process system. All of the units operated automatically by computer.

Prior to experiment, the packed column was evacuated by a high vacuum pump and purged with hydrogen. The required flow and the corresponding system pressure were adjusted with hydrogen and a sufficiently long time was allowed for the mass spectrometer until hydrogen mass fraction reached at more than 99.99%. Experimental conditions were represented in Table 3.

3.3 Process description

A two-bed six-step PSA process with equalization steps was used. In this kind of cycle, two columns are connected during certain steps. These steps have equal duration and column 2 is delayed by half cycle. The operation step time of a two-bed PSA system was shown in Table 4, and the flow patterns in the various phases of a PSA cycle are illustrated in Fig. 2. A typical six-step two-bed PSA process goes through the following steps:

1) Feed pressurization step: the column is pressurized with feed gas.
2) Adsorption step: a high pressure feed is supplied continuously to the column in which preferential adsorption of the more

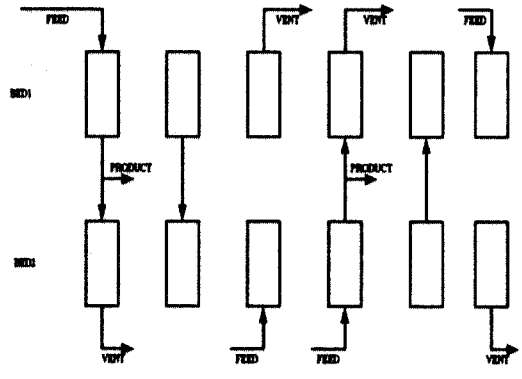

Fig. 2. 2-column 6-step PSA process cycle.

Table 4. 2-column 6-step PSA process step time sequence

	$k_1 \times 10^{-3}$	$k_2 \times 10^{-3}$	$k_3 \times 10^{-3}$	k_4	k_5	k_6	$Q[cal/mol]$
CH_4	2.43956	-0.00605	1.7585	1440.6	3.5026	-708.98	5625.18
H_2	1.6943	-0.0021	0.00625	1228.58	0.98	0.0	2880

strongly adsorbed components occurs; during this step, pure hydrogen is produced, a fraction of which is used to purge column 2.

3) Depressurizing equalization step: a high pressure feed is terminated and the bed is depressurized by transferring gas to the other bed through the product end.
4) Blowdown step: blowdown occurs in reverse flow direction, down to atmospheric pressure.
5) Purge step: a small fraction of the hydrogen produced by column 2 is expanded to low pressure, and used to purge column 1.
6) Pressurizing equalization step: the bed is repressurized from the product end using the depressurization gas from the other bed undergoing step 3.

4. Results and discussions

Equilibrium isotherms for methane and hydrogen gas were measured by the volumetric method at 293.15, 303.15 and 313.15K in the high-pressure equilibrium cell. As shownin Fig. 3, the results showed very high selectivity for methane over hydrogen at the range of experimental temperatures. And the experimental data fit very well to the Langmuir-Freundlich isotherm that was given by LRC model. The LRC model parameters were listed in Table 4.

Also, the isosteric heat of adsorption for each components were obtained by Clausius-Claypeyron equation, and represented in Table 5.

The adsorption dynamic characteristics of an adsorption column was studied, and the complete dynamic model described earlier was used to simulate the experimental data. As shown in Fig. 4, the slower the feed velocity, the longer the breakthrough time. Also, as the higher the pressure, the higher the adsorption capacity and the longer the breakthrough time became. And the breakthrough time did not decrease linearly according to the linear increase in the feed velocity. This implies that at least a certain amount of contact time was required due to the mass transfer resistance in the adsorbent. The predicted values fit quite well although the predicted exit concentrations of methane were lower than actual values. This is due to the use of hydrogen and its competition for the surface sites. Higher pressure will favor product purity of weak adsorbates but decrease the throughout or

Table 5. Loading ratio correlation model parameters for CH_4 and H_2 mixture onto activated carbon

FD	AD	DPE	BD	PU	PPE
20	300	20	20	300	20

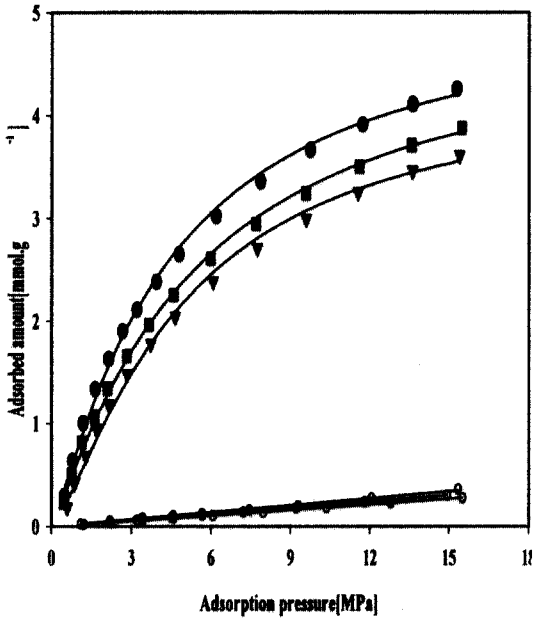

Fig. 3. Measured and fitted isotherms of CH_4 and H_2 onto activated carbon:●, 293.15K:■, 303.15K; ▼, 313.15K; —, L-F model.

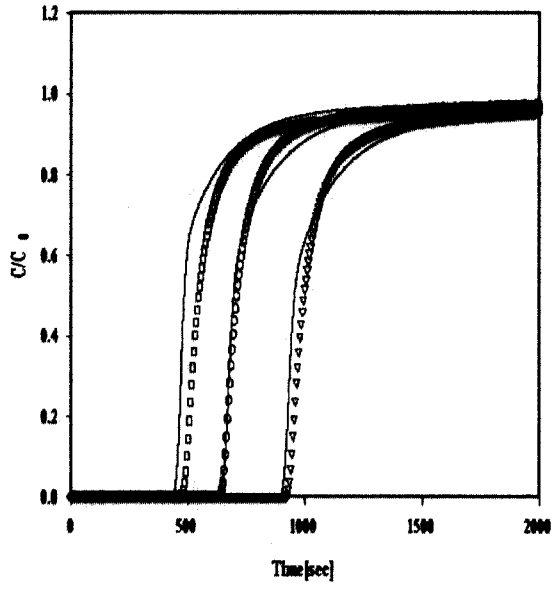

Fig. 4. CH_4 composition breakthrough curves for H_2/CH_4 system: ○, 11.8LPM feed rate at 8atm; □, 15.8LPM feed rate at 8atm; ▽, 11.8LPM feed rate at 12atm; —, LDF model.

productivity. The predicted values were lower than actual values as the same reason of the case of the effect of flow velocity. A breakthrough time could be defined as the time when the effluent concentration of the adsorbate reaches half of its inlet concentration.

4.1 The effect of flow rate

Appropriate feed rate is very important because it determines the throughput of the PSA process. The measured and predicted values of the hydrogen purity and recovery versus the flow rate at 11atm adsorption pressure and 0.0625 P/F ratio were shown in Fig. 5. The solid line was the predicted value. Hydrogen recovery and hydrogen purity were under 17LPM feed rate;, recovery and purity;, 8atm adsorption pressure;, 11atm adsorption pressure;, 13atm adsorption pressure;, 15atm adsorption pressure. treated as the dependent variables. The purity of hydrogen is represented by an average hydrogen concentration in the product leaving a column during the adsorption step. And the recovery of hydrogen is defined as the amount of hydrogen in net product over the amount of hydrogen in feed. The purity of hydrogen decreased with increasing flow rate since the portion of methane in a product stream increased. Otherwise, decreasing purity was the reason of the increasing a length of the mass transfer zone causing by increasing the superficial velocity. Increasing the feed rate, the experimental hydrogen recovery increased, but increasing feed rate might not be beneficial above certain feed rate.

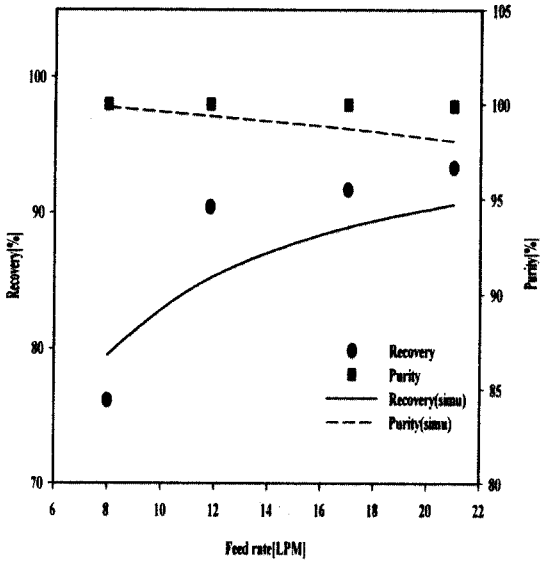

Fig. 5. Effect of Feed rate on H_2 purity and recovery for 2-column 6-step PSA process under 0.0625 P/F ratio and 11atm adsorption pressure.

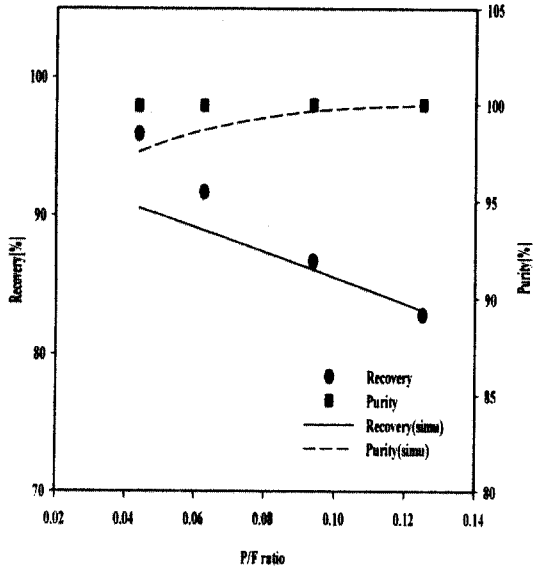

Fig. 6. Effect of P/F ratio on H_2 purity and recovery for 2-column 6-step PSA process under 17LPM feed rate and 11atm adsorption pressure.

4.2 The effect of P/F ratio

The P/F ratio is taken as the ratio of linear velocities or flow rates at their respective pressures. The purge step accomplishes an important function because it cleans the bed and prepares the bed for the next cycle, and consequently increases the hydrogen product purity. Generally, the product purity increases with the P/F ratio in an asymptotic manner, but a higher P/F ratio is not desirable because it lowers the product recovery of the weakly adsorbed component. Fig. 6 showed the measured and predicted values of the hydrogen purity and recovery versus the P/F ratio at 17LPM feed rate and 11atm adsorption pressure. The purity of hydrogen increased with increasing P/F ratio, but the hydrogen recovery decreased. At higher P/F ratios, the amount of hydrogen used to regenerate adsorbent increased so that itcould be possible to obtain high purity hydrogen, but which had the hydrogen recovery values reduced since it lowed in portion of hydrogen amount of product. Yang and Doong[35] stated a P/F ratio in the range of 0.06-0.08 is a likely optimal value in 50/50 hydrogen/methane system. And they stated when the P/F ratio further increased the hydrogen product purity will monotonically increase. However, the following adverse effects will arise: It will dilute the methane product, and will lower the hydrogen recovery. In this study, the optimal value to obtain more than 85% recovery and 99% hydrogenpurity was in the range of 0.07-0.10 P/F ratio at 17LPM feed rate and 11atm adsorption pressure.

4.3 The effect of adsorption pressure

The higher adsorption pressure results in

higher void and co-adsorbed hydrogen in the column at the start of the step, countercurrent depressurization, which is then lost during counter current desorption causing a larger reduction in hydrogen recovery by the process[31]. Raghavan and Ruthven[23]concluded that there is no real advantage in operating the PSA unit beyond a high operating pressure of about 18bar. Fig. 7 showed hydrogen purity and recovery over various adsorption pressure at 17LPM feed rate and 0.0625 P/F ratio. Increasing the adsorption pressure, hydrogen purity increased slightly but recovery decreased drastically because of a large reduction at blowdown step when adsorption pressure was high. And, operating above 11atm adsorption pressure might not be beneficial since the decreasing amount of hydrogen recovery increased comparing to increasing amount of hydrogen purity.

4.4 2-Column PSA process simulation results

Generally, higher hydrogen recovery and purity may be economic. When the separation factor is large, high recovery of purified high-pressure product is obtained and blowdown and purge losses are small. The simulation results of hydrogen recovery and purity for 2 columns and 6 steps PSA process under 17LPM feed rate was shown in Fig. 8. As shown that, increasing P/F ratio, hydrogen purity increased and recovery decreased, and increasing adsorption pressure, hydrogen recovery and purity had same manner of that. For the aspect of hydrogen recovery, adsorption pressure was appropriate above 11atm and below 13atm, and P/F ratio was

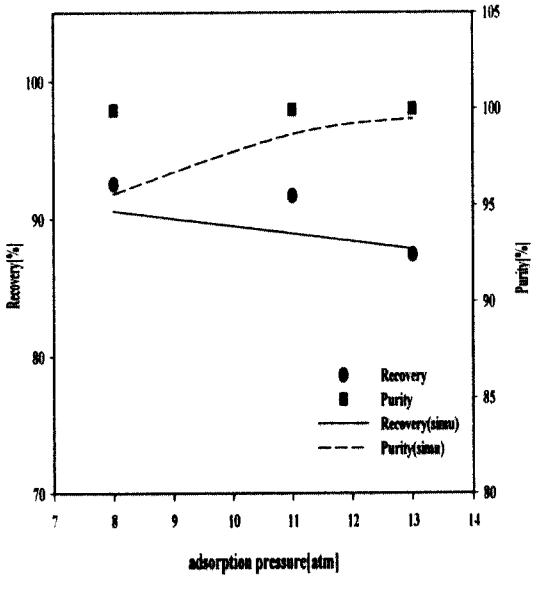

Fig. 7. Effect of adsorption pressure on H_2 purity and recovery for 2-column 6-step PSA process under 17LPM feed rate and 0.0625 P/F ratio.

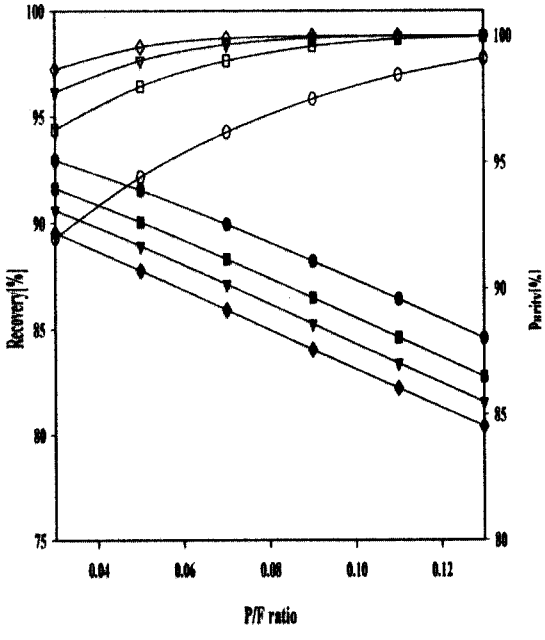

Fig. 8. Simulation results on H_2 recovery and purity for 2-column 6-step PSA process.

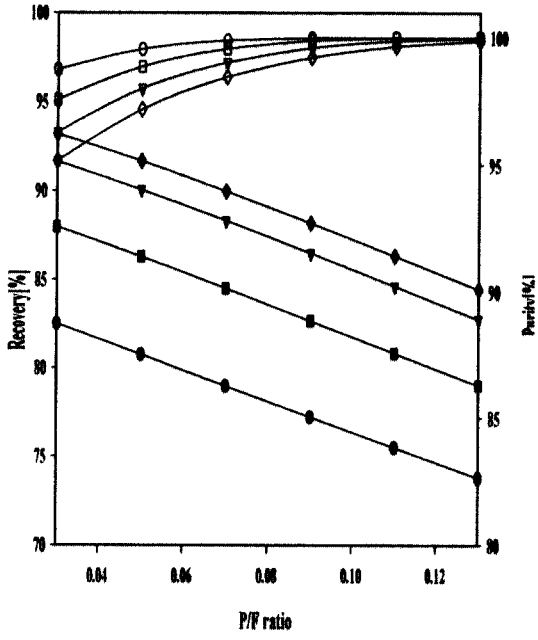

Fig. 9. Simulation results on H_2 recovery and purity for 2-column 6-step PSA process under 11atm adsorption pressure:, recovery and , purity; 8LPM feed rate;, 11.8LPM feed rate; 17LPM feed rate;, 21LPM feed rate.

appropriate the range of 0.07-0.10 to obtain more than 85% recovery. Also, for the aspect of hydrogen purity, adsorption pressure could be above 11atm and the above 0.07 P/F ratio to obtain more than 99% purity.

Fig. 9 showed the simulation results of hydrogen recovery and purity for 2-column 6-step PSA process under 11atm adsorption pressure. As shownthat, hydrogen recovery was reduced with increasing feed rate. Especially, the difference of amount recovery increasing decreased with feed rate and 17LPM feed rate was appropriate. But, hydrogen purity decreased monotonically with feed rate. For the aspect of P/F ratio, 0.07-0.1 P/F ratio might be appropriate for the object of this study. As a result, 17LPM feed rate, 11atm adsorption pressure and 0.07-0.1 P/F ratio might be optimal values.

5. Conclusions

A two-bed six-step PSA process with pressure equalization step was considered to study separation of hydrogen from hydrogen and methane(80/20) binary system onto activated carbon adsorbent on nonisothermal and nonadibatic condition. In the results of experiments, hydrogen recovery increased increasing feed rate, and decreasing adsorption pressure and P/F ratio. But, hydrogen purity increased decreasing feed rate, and increasing adsorption pressure and P/F ratio.In the results of simulation, 17LPM feed rate, 11atm adsorption pressure and 0.07-0.1 P/F ratio might be optimal values to obtain more than 85% recovery and 99% purity hydrogen.

Acknowledgment

This work was supported by LNG Technology Research Center, Korea Gas Corporation and Ministry of Commerce, Industry and Energy.

References

1) Ruthven, D. M.: "Principles of Adsorption and Adsorption Processes", John Wiley & Sons, New York(1984).
2) Ruthven, D. M., Farooq, S. and Knaebel, K. S.: "Pressure Swing Adsorption", VCH publishers, New York(1994).
3) Skarstrom, C. W.: U. S. Patent No. 2944627(1960).
4) Berlin, N. H.: U. S. Patent No. 3280536, 1996.

5) Marsh, W. D., Pramuk, F. S., Hoke, R. C. and Skarstrom, C. W.: U .S. Patent No. 3142547(1964).
6) Fuderer, A. and Rudelstorfer, E.: U.S. Patent No. 3846849, 1976.
7) Krzysztof W. and Marek, T.: Chem. Eng and Proc., Vol. 36, 1997, p. 89.
8) Malek, A. and Farooq, S.: AICHE J., Vol. 43, No. 10, 1997, p. 2509.
9) Malek, A. and Farooq, S.: AICHE J., Vol. 44, No. 9, 1998, p. 1985.
10) Park, J. H., Kim, J. N. and Cho, S. H.: AICHE J., Vol. 46, 2000, p. 790.
11) Pigorini, G. and Levan, M. D.: Ind. Eng. Chem. Res., Vol. 36, 1997, p. 2296.
12) Ahn H.. Lee, C. H., Seo, B., Yang, J.and Baek, K.: Adsorption., Vol. 5, 1999, p. 419.
13) Chan, Y. N.. Hill, F. B. and Wong, Y. H.: Chem. Eng. Sci., Vol. 36, 1981, p. 243.
14) Garg, D. R. and Ruthven, D. M.: Chem. Eng. Sci., Vol. 28, 1973, p. 799.
15) Garg, D. R. and Ruthven, D. M.: Chem. Eng. Sci., Vol. 29, 1974, p. 1961.
16) Garg, D. R. and Ruthven, D. M.: Chem. Eng. Sci., Vol. 29, 1974, p. 571.
17) Huang, C. C. and Fair, J. R.: AICHE J., Vol. 34, 1988, p. 1861.
18) Hwang, K. S., Jun, J. H. and Lee, W. K.: Chem. Eng. Sci., Vol. 50, No. 5, 1995, p. 813.
19) Sircar, S. and Kurma, R.: Ind. Eng. Chem. Process Des., Vol. 22, 1983, p. 271.
20) Malek, A. and Farooq, S. J.: Chem. Eng. Data., Vol. 41, 1996, p. 25.
21) Harwell, J. H., Liapis, A. I., Lichtfield, R. and Hanson, D. T.: Chem. Eng. Sci., Vol. 35, 1980, p. 2287.
22) Wong, Y. W. and Niedzwiecki, J. L.: AICHE Symp. Ser., Vol. 78, 1982, p. 219.
23) Kalu, B. K. and Sweed, N. H.: "Fundamentals of Adsorption", Eng. Foundation, New York(1984).
24) Myers, A. L. and Prausnitz, J. M.: AICHE J., Vol. 11, 1965, p. 121.
25) S. Qiao, K. Wang and X. Hu.: Langmuir., Vol. 16, 2000, p. 5130.
26) Yagi, S. and Kunii, D.: AICHE J., Vol. 6, No. 1, 1964, p. 97.
27) Suzuki, M.: "Adsorption Engineering", Elsevier, Amsterdam(1990).
28) Wakao, N. and Funazkri, T.: Chem. Eng. Sci., Vol. 33, 1978, p. 1375.
29) Yang, R. T.: "Gas Separation by Adsorption Processes", Butterworth, Boston, MA(1987).
30) Hoffman, K.A. and Chiang, S. T.: "Computational Fluid Dynamics for Engineers", A Publication of Engineering Education System, Wichita(1993).
31) Wu, J. C., Fan, L. T. and Erickson, L. E.: Comput. Chem. Eng,, Vol. 14, 1990, p. 679.
32) Yang, R. T. and Doong, S. J.: AICHE J. Vol. 31, 1985, p. 1829.
33) Yang, R. T. and Doong, S. J.: AICHE J., Vol. 32, 1986, p. 397.
34) Waldron, W. E. and Sircar, S.: Adsorption., Vol. 6, 2000, p. 179.
35) Raghavan, N. S. and Ruthven, D. M.: AICHE J., Vol. 31, No. 12, 1985, p. 2917.
36) Kunii, D. and Smith, J. M.: AICHE J., Vol. 6, No. 1, 1960, p. 71.